Mass-Losses Relationship in an Optimized 8 poles Radial AMB for Long Term Flywheel Energy Storage

L. S.Bakay, M. Dubois, and P. Viarouge
Department of Electrical Engineering
LEEPCI — Laval University
Quebec-City, CANADA
e-mail: loicq-serge.bakay.1@ulaval.ca

***Abstract* — This paper presents the effect of losses on a radial Active magnetic bearings (AMB), used in the Long Term Flywheel Energy Storage (LTFES). The study does not take into account the losses due to power electronics and windage losses (due to the friction between external rotor surface and the air). Therefore, we restricted the loss computation to those of radial AMB only. To simplify this work, we focused on the effect of external disturbance on unbalance force induced by rotor eccentricity for instance. The unbalance force has fixed the maximum radial load capacity of the rotor in order to design the radial AMB. 2-D Finite Element Method (FEM) has been used to validate the theoretical model. We have optimized AMB system in order to search the best design which minimises overall losses (Copper and iron Losses) for different magnitudes of external force. Then, mass versus losses curve of AMB has been shown for the same angular velocity speed of rotor namely 9000 rpm.**

Keywords- Active magnetic bearing, Long Term Flywheel Energy Storage, losses, optimization, weight

I. INTRODUCTION

Flywheels are increasingly used as a means for energy storage thanks to their capacity to store an important quantity of energy, their long lifetime and their large charge/discharge cycles [1]. They are spun up by a motor/generator drive depending of either charge or discharge instant of the flywheel. To store a large amount of energy, high speed composite materials are often used. Due to their high speed operation, contactless bearings are required in order to reduce the friction losses which are important in the flywheel applications. Fig. 1 shows example of an active magnetic bearing.

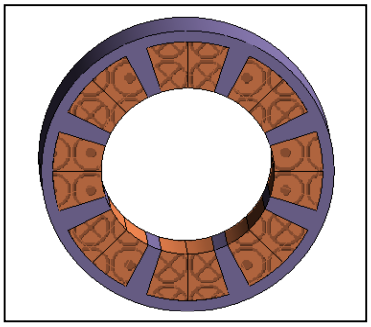

Fig. 1: Radial AMB geometry

Thanks to the absence of contact between rotating and non-rotating parts of a system, magnetic bearings system is used in the high speed rotating systems such as Flywheels and turbomachinery [2].

Flywheel stabilization is ensured by associating radial and axial bearings which act respectively radially and axially on the device. In the Long Term Flywheel Energy Storage fig.2, loss minimization of overall system is required. Therefore, the losses of each component (i.e. motor/generator, flywheel, magnetic bearing...etc.) of system must be minimized. In the case of the present work, we minimize AMB losses which considerably affect the radial AMB mass.

For the purpose of explaining and showing variation of the AMB weight for different unbalance force magnitude, the present work will be restricted on the AMB geometry only.

II. ROTATING MASS UNBALANCE

The response to a synchronous excitation, like unbalance, causes a synchronous whirling of the rotor; if the whole system is axi-symmetrical, a circular synchronous whirling occurs and produces radial forces, which are synchronous with the shaft rotational motion. This unbalance will cause synchronous vibrations in the two axes of the system which must be compensated by the two radial AMB.

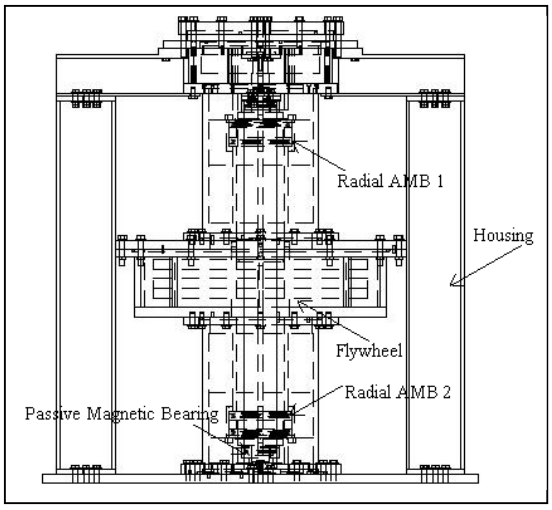

Fig.2: Flywheel assembly

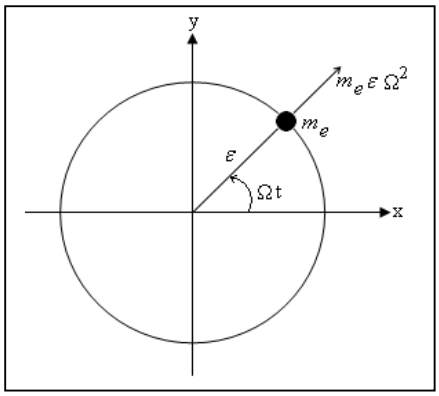

Fig. 3: Unbalance mass principle

These radial forces determine the force requirement of radial AMB. Therefore, AMB electromechanical devices have to take into account the disturbance flux flowing in the AMB core as well as the disturbance current in the coils. Fig. 3 shows the principle of unbalance force generation, where the shaft is considered as perfectly symmetrical but having an additional mass m_e at a radius of ε with an angle Ωt, where Ω is the rotational angular speed of the rotor. The Radial force is projected on the x-y axes as defined by [3].

$$F_x = m_e \varepsilon \Omega^2 \cdot Cos(\Omega t) \qquad F_y = m_e \varepsilon \Omega^2 \cdot Sin(\Omega t) \quad (1)$$

Amplitude of these forces is proportional to the square of rotational speed. Generally, m_e and ε are unknowns and depend on acceptable eccentricity of center of gravity ε specifications of the customer. In practice, maximum unbalance force is calculated as the product of unbalance U(g-mm) and the square of rotation speed Ω(rad/s) [4].

$$F_{\max} = U \cdot \Omega^2 \qquad U = \frac{G \cdot 60}{2 \cdot \pi \cdot n} \cdot m \quad (2)$$

Where m (g) is the mass, n (rpm) the rotation speed, and G (mm/s) the empirical balancing grade of the total system and depends on the quality of balancing. From (2), we can infer the maximum force F_{rmax} which acts on each radial AMB and which, with a security factor, will fix the design of the AMB.

$$F_{r\max} = \frac{U \cdot \Omega^2}{2} \quad (3)$$

Typical values of the balancing grade G are given in [5]. For a flywheel a typical value of G is 6.3 mm/s, which does not include the security factor.

III. Electromagnetic Model

A. Radial AMB specifications

The most common radial AMB geometries are those with three, four, six and eight poles.

The choice will depend on the application. Note that the use of three, four or six has an interaction between the poles, which makes their control more sophisticated. This study is limited to eight poles radial AMB geometry because it enables to easily control each electromagnet force independently.

Nevertheless, in eight poles radial AMB, four power amplifiers are required to drive the four currents flowing in the electromagnets, making them more expensive than three pole geometries for instance.

As we will see in section B, the electromagnetic force hardly depends on the geometric parameters such as tooth angle θ_d, inner diameter D and axial length L of the radial AMB as shown in fig. 4.

B. Radial force computation

In the theory of magnetic circuits, the generalized force calculation is given by the following magnetic co-energy formula.

$$\frac{\partial W'}{\partial e} = F_m \quad (4)$$

Where W' is the co-energy of system, e the air gap and F_m the electromagnetic force. Before calculating inductance for each electromagnet, we consider the magnetic circuit as linear and assume the relative permeability of material to be much higher than air. From these assumptions, inductance L_b (functions number of turns N of winding) can be computed as follows:

$$L_b = N^2 \cdot \frac{1}{2 \cdot \int_{Di/2}^{D/2} \frac{dr}{\mu_0 S(r)}} \quad (5)$$

Where S(r) is cross-section of the flux path in the airgap, from the tooth to the rotor laminations.

$$S(r) = r \cdot \theta_d \cdot L \quad (6)$$

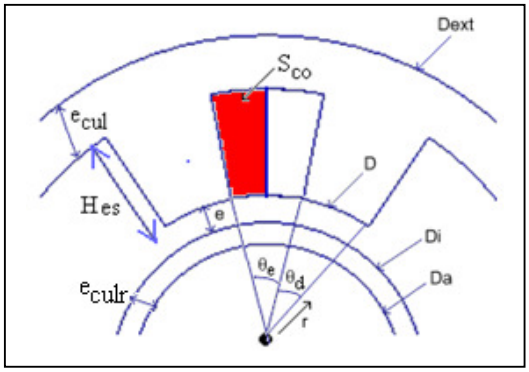

Fig. 4: Analysis model of Radial AMB

TABLE 1: Input data of radial AMB

AMB maximum Outer diameter	Dext	400 mm
Number of poles	8	∅
Coils turn (for each electromagnet)	100	∅
Air gap	e	1 mm
Flywheel shaft diameter	Da	100 mm
AMB maximum axial length	L	150 mm
Flywheel rotor mass	200	kg

In this paper, the maximum outer diameter Dext, and maximum axial length L have been fixed from the flywheel housing size and others parameters as shown in Table I.
Assuming that the AMB operates in the linear region of the laminations B(H) curve, energy and co-energy of the system are equal.
Energy of pole pair is located in the coil inductance only and can be written as (7) where *i* is the current flowing in the electromagnet.

$$W_m = \frac{1}{2} L_b i^2 = N^2 \cdot \mu_0 \theta_d L \cdot \ln\left(\frac{D}{D_i}\right)^{-1} i^2 \quad (7)$$

Equations (4) and (7) for each electromagnet become (8):

$$F_m = J^2 \cdot S_{co}^2 \cdot \mu_0 \theta_d L \cdot \frac{d}{de}\left(\ln\left(\frac{D}{D_i}\right)^{-1}\right) = k \cdot J^2 \quad (8)$$

J the current density and k is a factor taking into account the dimensions of AMB.

$$k \approx \alpha \cdot \frac{{S_{co}}^2 \cdot \mu_0 \cdot L \cdot (D/2) \cdot \theta_d}{e^2} Cos\left(\pi/8\right) \quad (9)$$

Wherein α is the winding *filling factor*.

The bearing current *i* is has two components: constant current I_0 for the purpose of ensuring stiffness of the rotor and sinusoidal current Δi allowing compensation of the peak value of disturbance force around the operating point I_0.Knowing that J_0 and ΔJ_{max} are respectively the currents density of current I_0 and Δi — which are related by S_{co} —, radial force F_m of AMB becomes (10):

$$F_m = k \cdot \left(J_0 + \Delta J_{\max}\right)^2 \quad (10)$$

In order to insure quasi-linear magnetic properties in the entire operating range, a maximum value of the magnetic flux density *Bmax* has be defined at the limit of linearity of B-H curve. Furthermore, the optimal operating point B_0 due to I_0 of the radial AMB is defined as half the value of the maximum magnetic flux density as shown in figure 5.

C. Losses assessment

While there is no mechanical friction in magnetic bearings, copper, iron and aerodynamic losses must be taken into account. These losses, which heat up the rotor, have to be extracted by the motor/generator drive [2], slowing down the flywheel.

1) Copper losses

Copper losses P_{co} depends on copper resistivity $\rho_{co,}$ copper volume V_{co} and current (both pre-magnetization and disturbance current) density J as shown in (11). They are located on the stator part of the AMB only.

$$P_{co} = \rho_{co} \cdot V_{co} \cdot \left(J_0 + \frac{\Delta J_{\max}}{\sqrt{2}}\right)^2 \quad (11)$$

From (9) we observe existence of constant losses even in the absence of any disturbance, caused by J_0.

2) Iron losses

The iron losses P_{iron} are due to a variety of mechanisms related to the fluctuating magnetic field and are located in both the stator and the rotor. In prior work, iron losses in the stator have been neglected [6] but they cannot be neglected in a long term energy storage application. To reduce aerodynamic losses resulting from aerodynamic drag, vacuum housing is often used. Usually, iron losses are divided into two components namely eddy currents losses P_{ed} and hysteresis losses P_h. To reduce eddy currents losses, laminated materials are usually used.

$$P_{iron} = P_h + P_{ed} \quad (12)$$

According to the Steinmetz relationship, measurement and computation of core mass losses are made with sinusoidal flux induction of magnitude B and frequency f often modeled by:

$$p_{iron} = k_h B^n f + k_{ed} B^2 f^2 \quad (13)$$

The coefficients k_h, k_{ed} and n depend on the laminated material, its thickness and conductivity.

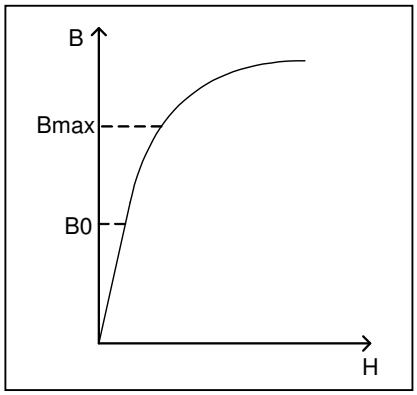

Fig 5: B-H material curve

IV. TOTAL AMB MASS COMPUTATION

In this section we calculate the total mass of radial AMB in order to make a relationship between the latter and the dimensions for the purpose of optimization of AMB device.

A. *Iron mass*

Iron mass is the sum of the both teeth, and the both stator and rotor yokes which are calculated by the iron mass density ρ_{iron} and volumes of different parts.

$$\begin{aligned} m_{teeth} &= \rho_{iron} \cdot V_{teeth} \\ &= 4 \cdot \rho_{iron} \cdot \theta_d \cdot L \cdot Hes \cdot (D + Hes) \end{aligned} \quad (14)$$

$$m_{syoke} = \rho_{iron} \cdot V_{syoke} = ecul \cdot L \cdot \pi \cdot (Dext - ecul) \quad (15)$$

$$m_{ryoke} = \rho_{iron} \cdot V_{ryoke} = eculr \cdot L \cdot \pi \cdot (Da + eculr) \quad (16)$$

$$m_{iron} = m_{teeth} + m_{syoke} + m_{ryoke} \quad (17)$$

B. *Copper mass*

Copper mass includes the end-winding volume and is calculated by (18), where ρ_{copper} is the copper mass density.

$$\begin{aligned} m_{copper} &= \rho_{copper} \cdot V_{co} \\ &= 4 \cdot \alpha \cdot S_{co} \cdot \left(L + \left(\frac{Dext - 2 \cdot ecul + D}{2} \right) \cdot \frac{\theta_d}{2} \right) \end{aligned} \quad (18)$$

Total mass is given by the sum of both mass copper and iron mass as presented in (19)

$$m_{tot} = m_{copper} + m_{iron} \quad (19)$$

V. VALIDATION AND RESULTS

In this section, validation and results of different simulations of radial AMB are presented. The software used for validation is MAGNET Finite Element Model.

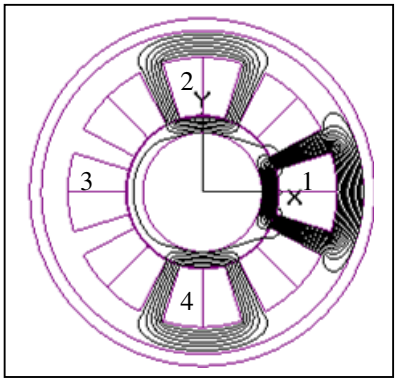

Fig.6: AMB Flux repartition at t=0

For the purpose of reducing eddy current losses, laminated material is often used. For this reason, Steel *M19-29 Ga* material has been chosen in both stator and the rotor laminations while the *304 Stainless steel* material has been chosen for the shaft.

Figure 6 shows the flux distribution through the cross-sections of the radial AMB at t = 0. The operation of this AMB is such that when the unbalance is located in front of electromagnet 3 (at t = 0), the sinusoidal current subtracts from the pre-magnetization current I_0 which decrease the total flux in electromagnet 3, and adds to electromagnet 1 to produce a force to overcome the unbalance force; that script is illustrated in figure 6. In the meantime, nothing occurs in y axis which keeps the current in the both electromagnets 1 and 2 equal to I_0. Note that the unbalance is assume as concentrated at one single rotor location.

Using the unbalance force described in (3) and flywheel data given in Table I, radial AMB is optimized in order to minimize losses. Figure 7 shows the variation of the total mass of different radial AMBs including the rotor laminations mass as function of unbalance maximum force amplitude for a 200 kg (440lbs) flywheel with a security factor 3. In Fig.7, to each point of the curve corresponds a single AMB design. Each AMB design is optimized for the nominal speed shown in Fig.7. With the use of (2) and (3), nominal speed and unbalance force are considered as directly related if the flywheel mass *m* is kept equal (here m = 200 kg) for each AMB design. Therefore, nominal speed and nominal AMB force can be presented on the same axis, as shown in Fig.7. The maximum unbalance force of whole system is (owing to two AMBs) twice higher than the one of each AMB. It is important to note that when the speed increases, unbalance force increases also according to (2). To overcome this disturbance force radial AMB mass increases also as shown in fig.7.

Energy in the flywheel storage system is proportional to the square of rotational speed as shown (20)

$$E = \frac{1}{2} J_f \Omega^2 \quad (20)$$

J_f is the inertia of the rotational mass and Ω the rotational speed of flywheel. To increase kinetic energy for a give mass, it is convenient to operate at high speed. Usually, owing to the peripheral limits of steel materials, composite materials are often used. Therefore, unbalance forces acted on AMB are important and their designs have to take them into account.

Figure 8 shows AMB mass variation as function of standby losses. A low level flywheel with large radius and having an amount of equivalent energy to a high-speed flywheel with short radius will have lower unbalance force, lower AMB mass and lower losses. Whence, self-discharge time for a high-speed bearing is shorter than for a low-speed bearing.

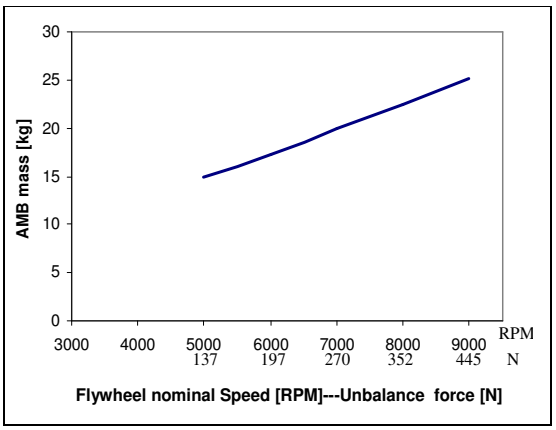

Fig.7: Variation of AMB mass versus unbalance force amplitude

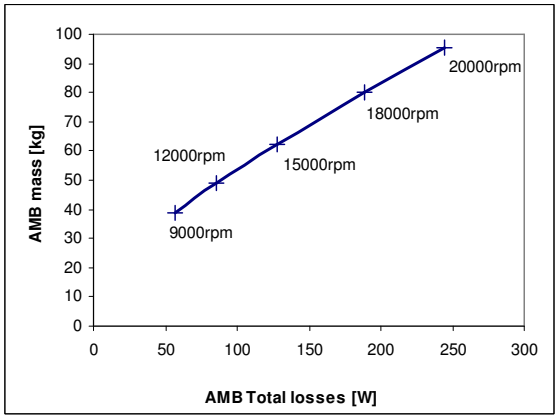

Fig.8: AMB mass versus total losses

VI. CONCLUSIONS

The radial Active Magnetic Bearing design was described, for the purpose of optimizing its losses in the case of an unbalance. We shown the losses effect in the radial AMB mass functions of rotational speed. We remarked the increase of AMB mass when rotational speed increases. However, in regard of the application, a compromise between losses and speed has to be made to ensure a good efficiency of overall system.

For a 39 kg AMB mass, we obtained 57W of total losses at 9000 RPM and for an 80 kg AMB mass, we obtained 188W at 18000 RPM. Therefore, for Long Term Flywheel Energy Storage, it is more suitable to operate the flywheel at low speed.

REFERENCES

[1] A. Palazzolo, D.Pang, D.K. "Extreme Energy Density Flywheel Energy Storage System for Space Applications" 6th International Energy Conversion Engineering Conference (IECEC) 28-30 July 2008, Cleveland, Ohio

[2] G.Schweitzer, H. Bleuler and A.Traxler, "Active Magnetic Bearings" Vdf Hochschlverlag AG an der ETH Zürich, 1994.

[3] A.Chiba,, T. Fukao, O. Ichikawa, M. Oshima, M. Takemoto and D.G Dorrell "Magnetic bearings and bearingless Drives" Newnes publications

[4] www.fr.schunk.com/schunk_files/attachments/Berechnung_Gesamtwuchtguete_EN_FR.pdf

[5] International Standard ISO 1940/1-1986 (E), "Mechanical vibration-Methods and criteria for the mechanical balancing of flexible rotors"

[6] H. Habermann, "Fonction guidage en rotation, Paliers magnétiques" Techniques de l'Ingénieur. Génie Mécanique Vol: BD3--1984